Turkish Online Journal of Qualitative Inquiry (TOJQI)
Volume 12, Issue 5, May 2021: 2157-2168

# Multiport Cuk Converter Using Solar With Battery Charging And Discharging Mode

Fayaz Ahamed.A [a], Kavipriya.G[b], Krithika.S [c], Naveena.S [d], Pooja.O [e]

[a,b,c,d,e]IV Year Electrical and Electronics Engineering, RMK Engineering college, Kavaraipettai

***Corresponding author:** [a] afd.eee@rmkec.ac.in, [b] kavi17136.ee@rmkec.ac.in, [c] krit17203.ee@rmkec.ac.in, [d]nave17212.ee@rmkec.ac.in, [e]pooj17221.ee@rmkec.ac.in

**Abstract**

Multi-output converters are currently being explored as an potential replacement to traditional DC-DC topologies, so that it will boom electricity density in low-power multiload packages. The system looks at a converter with a lift topology that may be customised to cuk `converter provide more than one output. The Converter which obtain multiple outputs incorporates two converters with identical front ends to supply power from one switch. A Buck converter can be used in conjunction with Cuk using this technique. This approach requires fewer switches and allows for the management and monitoring of all outputs. To generate a 12V and 48V bus, the proposed converter was used to interconnect with solar panel, battery, and house loads in a renewable power converter system. Since it substances a 12V battery and a 48V load bus, the converter can be used with a sun panel. When light strength is unavailable, the converter actions to a method in which the 48V bus is powered by the 12V battery

**Index Terms**: Solar energy, DC-DC converter

## 1. Introduction

This paper is mainly used for renewable sources of energy such as solar and wind. The sunlight gets converted into electricity by the solar. The produced voltage range might be low, so the converter circuits are used to raise the low voltage. A converter is a system that converts low voltage dc into high voltage dc. Power plants, home appliances,

ventilation systems, industrial appliances, solar lamps, vehicles, and other remote applications that include transmission and distribution use solar energy. In all of the conventional strategies, energy harvesting is generally achieved in steps, that is the maximum power extraction from an ambient electricity supply and DC-DC conversion. The impedance of an circuit ought to be regulated for optimal power extraction, making it hard to alter the output concurrently. A separate DC-DC converter is normally used after a most power extraction circuit, ensuing in a wide shape issue due to the presence of more than one inductor.

Several inputs and outputs are here where the rechargeable battery can be used as both. In battery charging mode, the rechargeable battery is charged by the residual energy where the harvested energy is greater than the load.

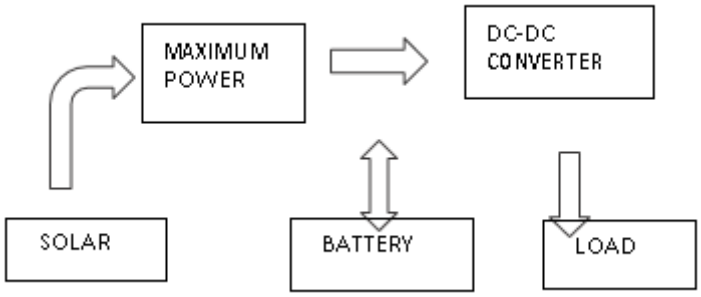


**Figure 1(a):**Block diagram of existing system

On-chip supplies for consumer electronic products, power supplies for consumer appliances, renewable energy integration in homes, and electric vehicles are some of the applications being studied for these converters.

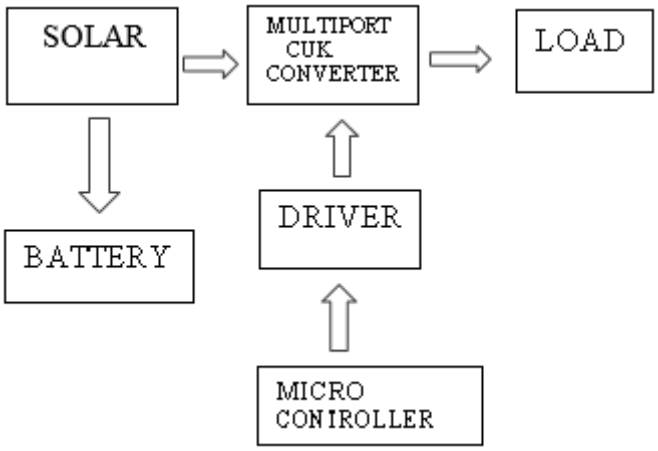


**Fig 1(b)** Multiport cuk converter based on solar energy

The battery must supply power to the load if the extracted energy is less than the load, which is known as battery discharging mode. The microcontroller is for generating pulses for converter circuit and pulses are given to the circuit as input. The driver circuit is specifically used to tolerate and amplify the controller's input signals. The key power circuit devices are connected to the amplified driver output. The operating method is actually selected between the battery charging and the battery discharging mode based on the harvested energy and the device load. The integral-charging scheme is used to maximize the power efficiency in both modes.

**2. Operation Principle And Method Of Control**

Multi-port converters are referred to as such because the same port serves as both an input and an output in many applications. For implementations, the outcome of this kind of converter might be increased or decreased than the supply voltage.

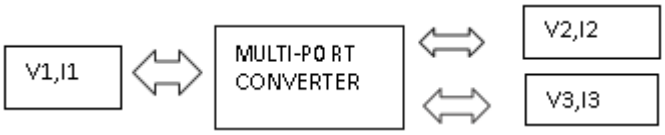


**Fig 2(a)** Block Diagram Of Multiport Cuk Converter

$$V1.I1+V2.I2+V3.I3=0$$

As in this equation, the current flowing through all ports is assumed to reach the positive terminal of the voltage at that port. When the voltage level remains constant, the output power and input current both rise. This criterion forces the input current to be higher since the source value is lower in a boost topology. As a consequence, running a multiport converter in continuous conduction mode is more effective.

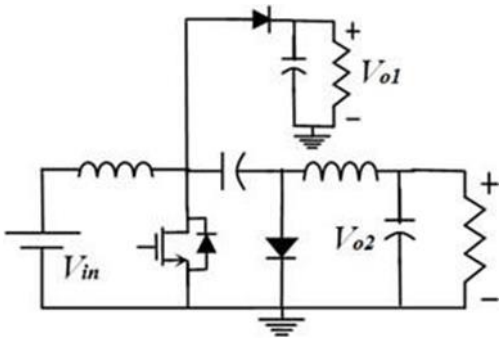


**Fig 2(b)** Multiport Converter Based On Boost And Cuk Topology

In managing their Integrated circuits, present communication and computation structures choose a voltage range that has to be greater or lesser than the supply input. Likewise, in electricity generation, a boost motor is coupled to a solar panel to enable a low operating voltage is being used to obtain a good Dc link. The charge sharing concept is used in turn increasing outputs. Figure 2 depicts a two-output boost topology developed using this approach (c). As an effect, the load is evenly distributed amongst these capacitors C1, C2 and so.

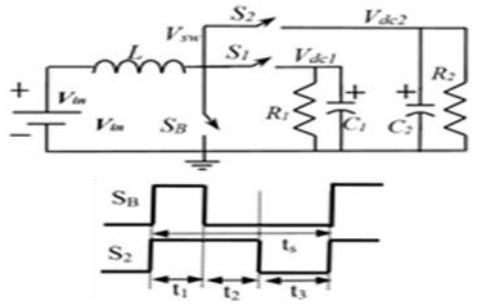


**Fig 2(c)** Conventional Switching Scheme And Multiport Converter With One Supply And Two Outputs.

As demonstrated, even under CCM, the data obtained are load-dependent. It's also significant to note that, unlike conventional boost converters, the voltage level can be lower than the input value. The endpoints in this form of multi-output converter exhibit extreme cross-regulation since all of the outputs are linked to the same switch node.

### A. Setup Overview

In rural roof-top solar power distribution, a multi-output cuk converter with switched boost action might be used. In this segment, a 24 V power source with dual outcomes is designed and validated as a test case. A 48 V bus connects the standard home loads. A 12 V output is fed to a battery with optimum charging (CC-CV) capabilities. The power switch has two modes of operation.

(i) MODE A: In CC-CV mode, 24V input supply power the 48V bus and charges the battery.

(ii)To simulate shading or night time conditions, the input supply is disconnected, and the 48 V bus is equipped with a 12 V battery.

### B. Mode a operation: interval 1:

In this mode, the input solar power supplies the loads on the 48V and the 12V output bus. On the 12-volt production path, the electrical feed charges the battery. The converter has three distinct intervals when operating in Mode-A. Figure 3 depicts the steady-state waveforms during the Phase-A service.

The analogous circuit for this interval is shown, in which the switches S1 and S2 are both turned on at the same time to allow the converter to boost. The current in inductor L1 increases as the slope of m1 (=Vin/L1) rises. The iL2, which has a gradient of m4 (=Vout2/L2), is freewheeled by S2. At this period, the toggle node voltages vsw1 and vsw2 are both shorted to the ground.

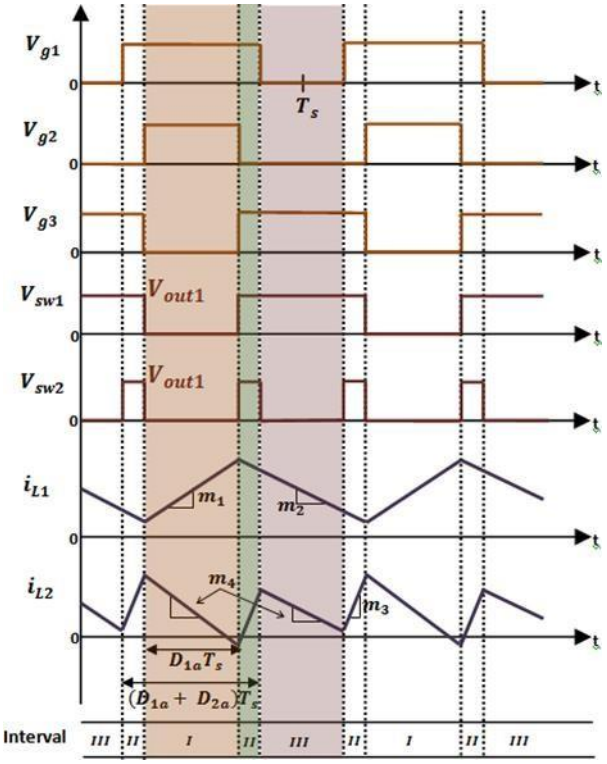


**Fig 3** Waveforms Of The Converter In Steady State Mode A

**Interval II:**

S2 is decided to turn off at this stage, while S3 is changed on and the diode is forward biased. The S1 is still turned on. In the boost scheme that was implemented, the inductance L1 discharges with a gradient of m2 and L2 begins loading with a slope of m3, leading in buck operation with 12V throughput at the battery end. The S2 is then ended up turning off, while the S3 is flipped on and the electrons flow. The S1 key hasn't been powered off yet.

The following is an examination of the correlation that has been applied:

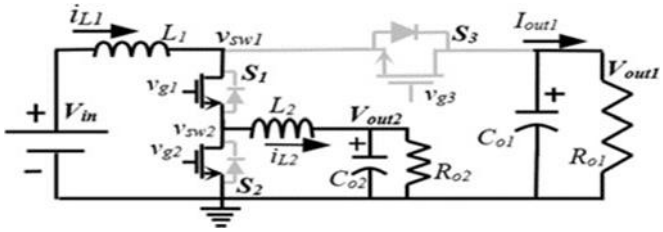


**Fig 4** Equivalent Circuit For Interval I

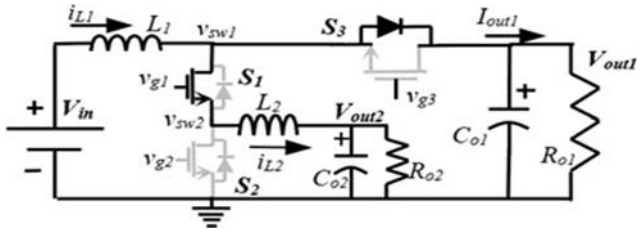


**Fig 5** Equivalent Circuit For Interval II

**INTERVAL III:**

Switch S1 is switched off during this interval. The interval in the analogous circuit is identical to the freewheeling mode of a traditional buck converter as shown in fig 6. The antiparallel diode, or switch S3, remains on. The current iL2 freewheels through the diode of S2 and has a slope of m4 as in sketch 1.

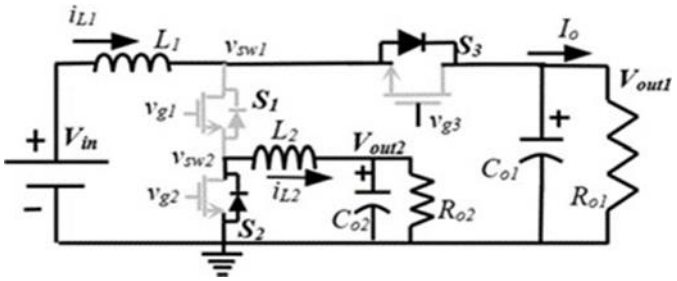


**Fig 6** Ideal Circuit For Interval III

**C. DESIGNING IN MODE A:**

**1) MODEL OF STEADY STATE:**

This part describes the steady-state voltage conversion ratio for all outputs. When you apply volt-sec balance across L1, you get,

Vin.D1a + (Vin - Vout1).(1 - D1a)=0

where D1a is the fraction of time when both S1 and S2 are turned on at the same time. As a consequence, the boost output voltage is

$$Vout1 = \frac{1}{1-D1a}. Vin$$

A volt-sec balance is extended through the inductor L2 to find an expression for Vout2.

-Vout2.D1a+(Vout1-Vout2).D2a

+(-Vout2).(1-D1a-D2a)=0

When only S1 is turned on, D2a is the fraction of the interval. As a result, the steady state expression for Vout2 is

$$Vout2 = \frac{D2a}{1-D1a} . Vin$$

**2)DYNAMIC MODEL:**

The generalised state space equation for circuit intervals described in mode A can be written as

$$J * x(t) + k * u=x(t) (t)$$

x(t) is a vector that contains all of the state variables, which are the inductor currents iL1, iL2 and capacitor voltages Vout1, Vout2. The independent input Vin is defined by u(t).

x(t) = [IL1 IL2 Vout1 Vout2]^T and u(t) = Vin During interval-1, above equation can be written as

$$x(t) = J1 * x(t) + k1 * u(t)$$

$$\text{Here, } J1= \begin{vmatrix} 0 & 0 & 0 & 0 \\ 0 & 0 & 0 & \frac{-1}{L2} \\ 0 & 0 & \frac{-1}{C01R01} & 0 \\ 0 & \frac{1}{C02} & 0 & \frac{-1}{C02R02} \end{vmatrix}, K1= \begin{vmatrix} \frac{1}{L1} \\ 0 \\ 0 \\ 0 \end{vmatrix}$$

During Interval II, x(t) = J2 * x(t) + k2 * u(t)

$$,J1= \begin{vmatrix} 0 & 0 & 0 & 0 \\ 0 & 0 & 0 & \frac{-1}{L2} \\ 0 & 0 & \frac{-1}{C01R01} & 0 \\ 0 & \frac{1}{C02} & 0 & \frac{-1}{C02R02} \end{vmatrix} ,K1= \begin{vmatrix} \frac{1}{L1} \\ 0 \\ 0 \\ 0 \end{vmatrix}$$

During Interval III, x(t) = J3 * x(t) + k3 * u(t)

$$J1= \begin{vmatrix} 0 & 0 & 0 & 0 \\ 0 & 0 & 0 & \frac{L2}{} \\ 0 & 0 & \frac{-1}{C01R01} & 0 \\ 0 & \frac{1}{C02} & 0 & \frac{-1}{C02R02} \end{vmatrix} ,K1= \begin{vmatrix} \frac{1}{L1} \\ 0 \\ 0 \\ 0 \end{vmatrix}$$

The data is annoying, and state-space averaging is used to calculate the average. With d1 and d2 as control variables, the final position stability analysis calculation is performed.

$$x = [sI - J]^{-1} * [K * u(s) + (J1 - J3) * X(s) * d1a(s) + (J2 - J3) * X(s) * d2a(s)]$$

$$J= \begin{vmatrix} 0 & 0 & \frac{-(1-D1a)}{L1} & 0 \\ 0 & 0 & \frac{D2a}{L2} & \frac{-1}{L2} \\ \frac{(1-D1a)}{C01} & \frac{(-D2a)}{C01} & \frac{-1}{C01R01} & 0 \\ 0 & \frac{1}{C02} & 0 & \frac{-1}{C02R02} \end{vmatrix} K= \begin{vmatrix} \frac{1}{L1} \\ 0 \\ 0 \\ 0 \end{vmatrix}$$

The control-to-output transition function can be plotted using the equation Vout1 / d1a.

## D. MODE B OPERATION:

The solar input is absent in Mode B. The loads are powered by the 12V battery. As a result, the pulses were changed to enable boost operation from a 12V battery to a 48V output bus. In this mode, the PWM signal to S1 is disabled. The converter's steady state waveforms during mode B operation. In a switching cycle, intervals are of two types.

### INTERVAL I:

Switch S2 is enabled at the onset of this timeframe. With a slope of m5, the inductor iL2 is loaded. The switch S3 has been switched off. When S2 is flipped on and L2 is charged to an input signal, this interval is analogous to boost operation.

Switch S2 is shut off and switch S3 is flipped on at the begin of this duration. With a decreasing slope of m6, the inductor L2 begins supplying energy to the 48V bus. This interval's corresponding circuit is shown in Fig.9. It's worth remembering that the voltage through Cin is Vout1 in steady state, so the current through L1 is zero.

**INTERVAL II:**

Switch S2 is shut off and switch S3 is flipped on at the begin of this duration. With a decreasing slope of m6, the inductor L2 begins supplying energy to the 48V bus. This interval's corresponding circuit is shown in Fig.9. It's worth remembering that the voltage through Cin is Vout1 in steady state, so the current through L1 is zero

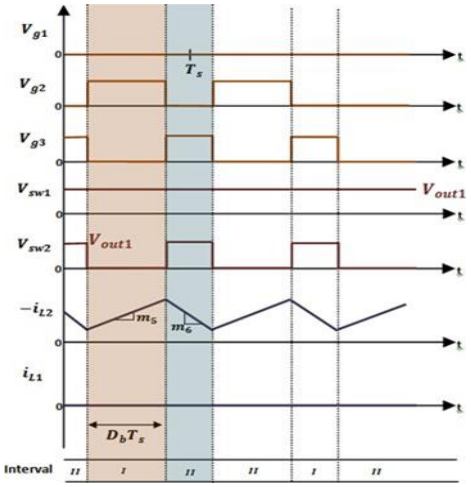


**Fig 7** Frequency Modulation Of The Amplifier In Focused In Type B

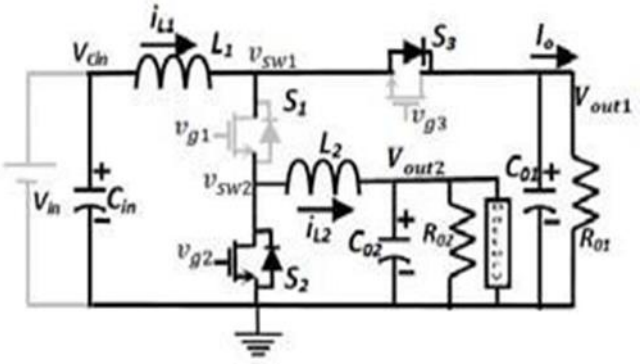


**Fig 8** Estimation Circuit For Interval I

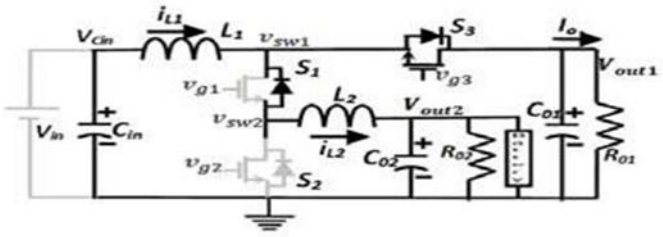


**Fig 9**equivalent Circuit For Interval II

**E. DESIGNING IN MODE B :**

**1) MODEL OF STEADY STATE :**

This section calculates the output Vout1's steady state power flow ratio.

-Vout2.DbTs +-Vout2.DbTs+-Vout2.DbTs+-Vout2.DbTs+-Vout2.DbTs+-V (Vout1 - Vout2).D'bTs = 0

Db is the percentage of time that S2 is switched on during the switching phase. As a consequence, the boost voltage rate will decrease.

$$\frac{Vout1}{Vout2} = \frac{Vout1}{battery} = \frac{1}{1-Db}$$

**2) DYNAMIC MODEL:**

For circuit intervals defined in mode B, the generalised state-space equation can be written as

$$P * x(t) + Q * u = x(t)\ (t)$$

u(t) is a independent input E, and x(t) is a vector that contains all of the random variables, which are inductor currents iL1, iL2 and capacitor voltages Vout1, Vout2, Vin.

During cycle 1,

$x(t) = [iL1\ iL2\ Vout1\ Vout2]T$ and $u(t) = E$

$$P1 * x(t) + Q1 * u = x(t)\ (t)$$

$$P1 = \begin{vmatrix} 0 & 0 & \frac{-1}{L1} & 0 & \frac{1}{L1} \\ 0 & 0 & 0 & \frac{-1}{L2} & 0 \\ \frac{1}{C01} & 0 & \frac{-1}{C01R01} & 0 & 0 \\ 0 & \frac{1}{C02} & 0 & \frac{-(R02+Rb)}{C02R02Rb} & 0 \\ \frac{-1}{Cin} & 0 & 0 & 0 & 0 \end{vmatrix}, \quad Q1 = \begin{vmatrix} 0 \\ 0 \\ 0 \\ \frac{1}{C02Rb} \\ 0 \end{vmatrix}$$

During Interval II,

$$P2 * x(t) + Q2 * u = x(t)\ (t)$$

Here,

$$P2 = \begin{vmatrix} 0 & 0 & \frac{-1}{L1} & 0 & \frac{1}{L1} \\ 0 & 0 & \frac{1}{L2} & \frac{-1}{L2} & 0 \\ \frac{1}{C01} & \frac{-1}{C01} & \frac{-1}{C01R01} & 0 & 0 \\ 0 & \frac{1}{C02} & 0 & \frac{-(R02+Rb)}{C02R02Rb} & 0 \\ \frac{-1}{Cin} & 0 & 0 & 0 & 0 \end{vmatrix}, \quad Q2 = \begin{vmatrix} 0 \\ 0 \\ 0 \\ \frac{1}{C02Rb} \\ \end{vmatrix}$$

Applying feature vector averaging to these intervals for minor perturbations in input u and control variable Db yields the final steady-space linearized equation.

$x = [ s1 - P]^{-1} * [Q * u(s) + (P1 - P2) * X(s) * db(s)]$

Here,

$$P=\begin{vmatrix} 0 & 0 & \frac{-1}{L1} & 0 & \frac{1}{L1} \\ 0 & 0 & \frac{(1-Db)}{L2} & \frac{-1}{L2} & 0 \\ \frac{1}{C01} & \frac{-(1-Db)}{C01} & \frac{-1}{C01R01} & 0 & 0 \\ 0 & \frac{1}{C02} & 0 & \frac{-(R02+Rb)}{C02R02Rb} & 0 \\ \frac{-1}{Cin} & 0 & 0 & 0 & 0 \end{vmatrix} \quad Q=\begin{vmatrix} 0 \\ 0 \\ 0 \\ \frac{1}{C02Rb} \\ 0 \end{vmatrix}$$

The control-to-output conversion function Vout1/db can be plotted using the equation

**F. OPTIMAL BATTERY CHARGING CONTROL:**

Recognize Fig. 10 for a summary of the CC-CV charging mode. (a), which defines a standard experimental optimised storage of batteries, where the device is assigned with a static current when its state-of-charge (SOC) is low and involved with a fixed value when its SOC is near 100%. Figure 10 illustrates a typical charge controller. An internal current loop and an outer voltage loop are also found in the unit. The voltage compensator's performance is clamped by a Zener diode. When the cell SOC is close to zero (VbatVref), it is held in place to Vz, which sets the circuit reference to Vz. This is visualized in fig 11(a).

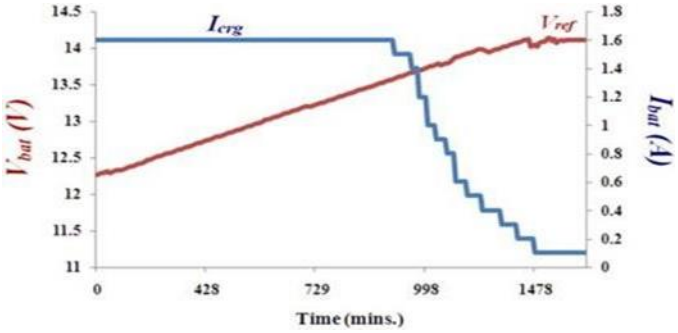


**Fig 10(a)** Characteristics Of Optimal Charging Batteries

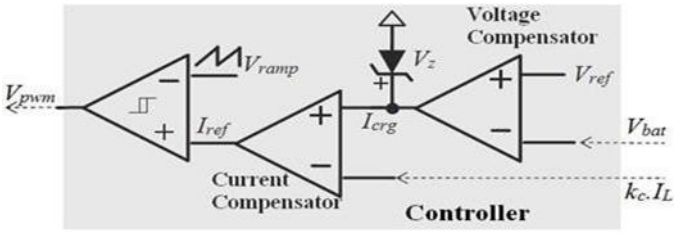


**Fig 10(b)**A monitoring circuit for simple optimal battery power

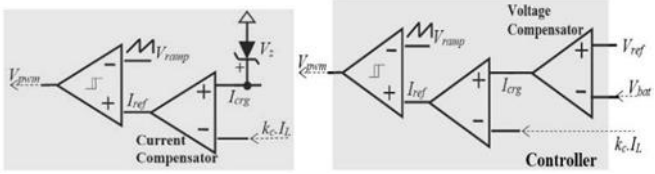


**Fig 11(a) & (b)** architecture of the control algorithm in different battery state of charge(a) as a fixed current controller (b) as a dc link controller

## G. CONTROLLER OPERATION IN DIFFERENT MODES:

The power stage functions similarly to the previous sections. The converter's framework is described in two configurations in this chapter. Analogue controllers are being used to track the 48V and 12V outputs. A control circuit (control #1) regulates the boost output (Vout1) to 48V. Control #2 directs the step-down output (Vout2), which is linked to a battery. As per Figure 10.b), it is governed by a battery's precise charging order. Physical PWM controllers have been used for gathering all controller output signals, making the voltage level for S1 and the 48 V for S2 easier to attain. Based on the magnitude, a mode selection circuit alters the power between Mode A and Mode B.

## 3..Experimental Results:

In a sustainable energy switching cycle, this ingenious converter was used to link a components mentioned previously. The 12 V bus is wired to the battery and it is capable of powering it efficiently. During Mode, A functioning, the input source (Vin) will provide both outputs. The control shifts to another control when it is energized, which governs the output. As early as the setup is triggered at t1, the input source and the batteries continues to charging and bringing to Vout1.

Until the battery is the origin in mode B, the control only enforces Vout1 at 48 V. Among both t1 and t2, the electrode existing (Iout2) charges the 48 V output. After t2, it maintains a stable state. The changeover from Mode A to Mode B is imposed by running the converter in Mode A and lessening the input source voltage. The mode selector informs the converter again to use the battery to drive the 48 V load. The input source is loading the battery and allocating the 48 V bus before t1, and that's because of the direction of IL2. To initiate the shift from Mode A to Mode B, the input voltage is reduced at t1. The controller responds to the toggle to Mode B at a specific frequency t2. As a direct consequence, the current through L2 (=IL2) inverts its path. The battery resistivity at this place measures how much Vout2 has fallen. There will be a temporary drop in the 48 V bus at this transformation phase. The loss is analysed by the feedback loop's speed and the bus storing capacitor. After t3, the voltage level is estimated and moved to Mode B. The multi-port device could be said to set up as a solar array with a 12 V supply and a 48 V load bus, with all outputs being possible.

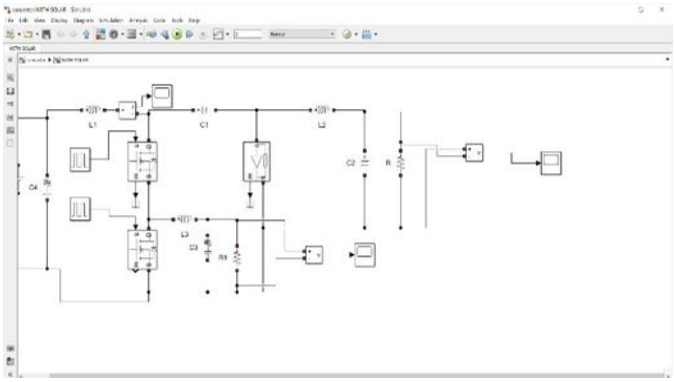

**Fig 12** Simulation Circuit With Solar Energy Harvesting

**Fig 12(a)** Output Waveform For Load

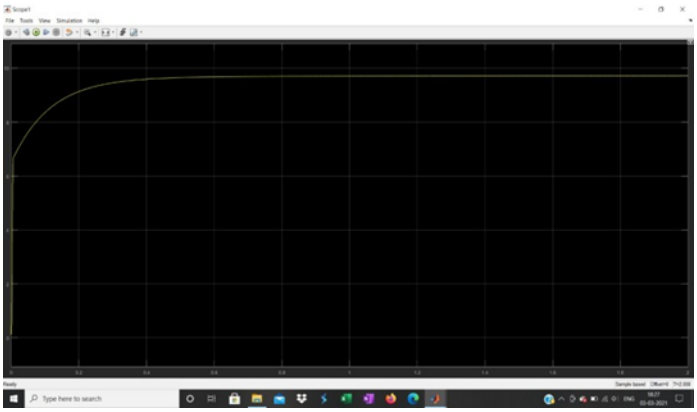

**Fig 12**(b) OUTPUT WAVEFORM FOR BATTERY

## 4. Conclusion:

A multi-port converter absorbs energy from a solar cell and converts it to DC. The multi-port converter automatically switches between battery charging and discharging mode based on the load current and extracted electricity. In the load current and extracted energy, the battery's charging time and discharging time are adaptively regulated and ensuring a slight output ripple in one switching cycle. A solar panel and a lithium ion battery were used to test the multi port cosnverter utilised before

## References


[1] IEEE Sensors Journal, vol.13, no.10, October 2013, pp. 3846-3853.

[2] Rong-Jong Wai and Jun-Jie Liaw, "High-Efficiency-Isolated-Single-Input-Multiple-Output Bidirectional Converter," IEEE Transactions On Power Electronics, Vol. 30, No. 9, Sept. 2015, pp. 4914-4930.

[3] S. Jeong, Z. Foo, Y. Lee, J. Y. Sim, D. Blaauw, and D. Sylvester, "A fully-integrated 71nW CMOS temperature sensor for low-power wireless sensor nodes," IEEE Journal of Solid-State Circuits, vol. 49, no. 8, pp. 1682-1693, August 2014.

[4] D. Ma, W.-H. Ki, C. Y. Tsui, and P. K. T. Mok, "Single-inductor multiple-output switching converters with time-multiplexing control in discontinuous conduction mode," IEEE J. Solid-State Circuits, vol. 38, no. 1, Jan. 2003, pp. 89–100.

[5] M. E. E. Alahi, L. Xie, S. Mukhopadhyay, and L. Burkitt, "A temperature compensated smart nitrate-sensor for agricultural industry," IEEE Trans. Industrial Electronics, vol. 64, no. 9, September 2017, pp. 7333-7341.

[6] Hyun-Chang Kim, Chang Soo Yoon, "A Single-Inductor, Multiple-Channel Current-Balancing LED Driver for Display

[7] Backlight Applications," Industry Applications, Vol. 50, No. 6, November 2014, pp. 4077-4081.

[8] R. J. M. Vullers, R. van Schaijk, I. Doms, C. Van Hoof, and R. Mertens, "Micropower energy harvesting," Solid-State Electron, vol. 53, no. 7, July 2009, pp. 684-693.

[9] "Battery-assisted and Photovoltaic-sourced Switched-inductor CMOS Harvesting Charger– Supply," .

[10] "A 3.4 mW photovoltaic energy-harvesting charger with integrated maximum power point monitoring and battery management,"

[11] H. Shao, X. Li, C. Y. Tsui, and W. H. Ki, "A novel single-inductor dual-input dual-output DC-DC converter with PWM control for solar energy harvesting,"

[12] H. Kim, Y. J. Min, C. H. Jeong, K. Y. Kim, C. Kim, and S. W. Kim, "A 1-mW solar-energy-harvesting circuit using an adaptive MPPT with a SAR and a counter," IEEE Trans. Circuits Syst. II: Exp. Briefs, vol. 60, no. 6, June 2013, pp. 331-335.

[13] Y. Qian, H. Zhang, Y. Chen, Y. Qin, D. Lu, "A SIDIDO DC–DC converter with dual-mode and programmable-capacitor-array MPPT control for thermoelectric energy harvesting,"August 2017.

[14] Y. Qiu, C. V. Liempd, B. O. H. Veld, P. G. Blanken, and C. V. Hool, "5-to-10mW input power range inductive boost converter for indoor photovoltaic energy harvesting with integrated maximum power point tracking algorithm," 2011.

[15] G. A. Rincon-Mora and R. D. Prabha, "0.18-m light-harvesting battery-assisted charger-supply CMOS system," April 2016.

[16] "A Pseudo-CCM/DCM SIMO Switching Converter with Freewheel Switching,"

[17] Changsik Yoo, Moon, "Load-Independent Current Control Technique of a Single-Inductor Multiple-Output Switching DC–DC Converter," Jan. 2012.

[18] Philip K. T. Mok and Xiaocheng Jing, "Power Loss and Switching Noise Reduction Techniques for Single-Inductor Multiple-Output Regulator," Oct 2013.

[19] D. Ma, W.-H. Ki, and C.-Y. Tsui, "A pseudo-CCM/DCM SIMO switching converter with freewheel switching," (June 2003).

[20] Pradipta Patra, Jyotirmoy Ghosh, "Control Scheme for Reduced Cross-Regulation in Single-Inductor Multiple-Output DC–DC Converters," Nov. 2013.

[21] A. T. L. Lee, and S. Y. Hui, "Buck-boost single-inductor multiple-output high-frequency inverters for medium-power wireless power transfer,"(April 2019).

[22] A. Kwasinski, "A modified-time-sharing switching technique for multiple-input dc–dc converters," Nov. 2012.

[23] Y. J. Moon, Y. S. Roh, J. C. Gong, and C. Yoo, "Load-independent current control technique of a single-inductor multiple-output switching DC-DC converter," .

[24] Ke-Horng Chen, "Single-Inductor Multi-Output (SIMO) DC-DC

[25] Converters with High Light-Load Efficiency and Cross-Regulation for Portable Devices,"April 2009.

[26] Venkata Kanamarlapudi, and colleagues, "A Digital Method of Power-Sharing and Cross-Regulation Suppression for Single-Inductor Multiple-Input Multiple-Output DC–DC Converter," .

[27] "New Single Input, Multiple Output Converter Topologies," in IEEE Industrial Electronics Magazine, June 2016, pp. 6-20, by Maria Bella Ferrera Prieto, Salvador Pérez Litrán, Eladio Durán Aranda, and Juan Manuel Enrique Gómez.